Identification of molecular candidates which regulate calcium-dependent CD8+ T-cell cytotoxicity

Sylvia Zöphel [a,1], Gertrud Schäfer [a,2], Maryam Nazarieh [b,3], Verena Konetzki [a,4], Cora Hoxha [a,5], Eckart Meese [c,6], Markus Hoth [a,7], Volkhard Helms [b,8], Mohamed Hamed [d,9], Eva C. Schwarz [a,*,10]

[a] Biophysics, Center for Integrative Physiology and Molecular Medicine, School of Medicine, Saarland University, Building 48, 66421 Homburg, Germany
[b] Center for Bioinformatics, Saarland Informatics Campus, Saarland University, 66041 Saarbrücken, Germany
[c] Human Genetics, School of Medicine, Saarland University, Building 60, 66421 Homburg, Germany
[d] Institute for Biostatistics and Informatics in Medicine and Ageing Research, Rostock University Medical Centre, 18057 Rostock, Germany

ARTICLE INFO

ABSTRACT

Cytotoxic CD8+ T lymphocytes (CTL) eliminate infected cells or transformed tumor cells by releasing perforin-containing cytotoxic granules at the immunological synapse. The secretion of such granules depends on Ca^{2+}-influx through store operated Ca^{2+} channels, formed by STIM (stromal interaction molecule)-activated Orai proteins. Whereas molecular mechanisms of the secretion machinery are well understood, much less is known about the molecular machinery that regulates the efficiency of Ca^{2+}-dependent target cell killing. CTL killing efficiency is of high interest considering the number of studies on CD8+ T lymphocytes modified for clinical use. Here, we isolated total RNA from primary human cells: natural killer (NK) cells, non-stimulated CD8+ T-cells, and from *Staphylococcus aureus* enterotoxin A (SEA) stimulated CD8+ T-cells (SEA-CTL) and conducted whole genome expression profiling by microarray experiments. Based on differential expression analysis of the transcriptome data and analysis of master regulator genes, we identified 31 candidates which potentially regulate Ca^{2+}-homeostasis in CTL. To investigate a putative function of these candidates in CTL cytotoxicity, we transfected either SEA-stimulated CTL (SEA-CTL) or antigen specific CD8+ T-cell clones (CTL-MART-1) with siRNAs specific against the identified candidates and analyzed the killing capacity using a real-time killing assay. In addition, we complemented the analysis by studying the effect of inhibitory substances acting on the candidate proteins if available. Finally, to unmask their involvement in Ca^{2+} dependent cytotoxicity, candidates were also analyzed under Ca^{2+}-limiting conditions. Overall, we identified four hits, CCR5 (C-C chemokine receptor type five), KCNN4 (potassium calcium-activated channel subfamily N), RCAN3 (regulator of calcineurin) and BCL (B-cell lymphoma) 2 which clearly affect the efficiency of Ca^{2+} dependent cytotoxicity in CTL-MART-1 cells, CCR5, BCL2, and KCNN4 in a positive manner, and RCAN3 in a negative way.

[1] https://orcid.org/0000-0001-7601-8889
[2] https://orcid.org/0000-0001-5159-0539
[3] https://orcid.org/0000-0001-8055-1838
[4] https://orcid.org/0000-0001-7936-7937
[5] https://orcid.org/0000-0002-3016-5119
[6] https://orcid.org/0000-0001-7569-819X
[7] https://orcid.org/0000-0001-7080-4643
[8] https://orcid.org/0000-0002-2180-9154
[9] https://orcid.org/0000-0002-9102-8839
[10] https://orcid.org/0000-0002-6503-4864

1. Introduction

Cytotoxic CD8$^+$ T lymphocytes (CTL) and natural killer (NK) cells eliminate infected or transformed tumor cells to control the integrity of the human body. Their main cytotoxic mechanism is the release of perforin/granzyme-containing lytic granules (LG) at the immunological synapse. LG release requires Ca^{2+} entry across the plasma membrane by STIM-activated Orai channels (Maul-Pavicic et al., 2011). Beside these key players, Ca^{2+} transporters and other ion channels such as TRPs, CaV, P2X receptors, and Piezo channels contribute to the regulation of Ca^{2+}-dynamics and Ca^{2+}-homeostasis inside cells (Feske et al., 2012; K. S. Friedmann et al., 2019; Trebak and Kinet, 2019). However, their roles for killer cell functioning are not completely understood and controversially discussed (Badou et al., 2013; Fenninger and Jefferies, 2019; Feske, 2013; Nohara et al., 2015; Pelletier and Savignac, 2013). The function of STIM and Orai proteins is, in principle, well understood and originated from data on severe combined immunodeficiency (SCID) patients, whereas our understanding of further proteins often relies on experimental data from human T-cell lines, mice, or various other cell lines. We have recently shown that there is an optimal Ca^{2+} concentration for primary human CTL-killing (approximately 25–600 μM of external Ca^{2+} concentration) (X. Zhou et al., 2018) that is far below the free Ca^{2+} concentration in peripheral blood (around 1.3 mM). However, the molecular machinery behind the optimal Ca^{2+} concentration that regulates Ca^{2+} dependent cytotoxicity remains unknown.

Over the last 15 years, small interfering RNA (siRNA) based screening strategies have advanced significantly and the therapeutic use of siRNA has been pushed forward as well (Hattab and Bakhtiar, 2020; Mainini and Eccles, 2020; Moffat and Sabatini, 2006; L. Y. Zhou et al., 2019). In primary human cells, RNAi transfection in naïve B-cells results in knockdown efficiencies of about 40–60% (Shih et al., 2019). In addition, optimized protocols for other primary immune cells (T-cells, monocytes, dendritic cells) were published (Mantei et al., 2008; Sioud, 2020; Smith et al., 2016). Numerous studies reported successful screens for the function of immune killer cells by siRNA-based approaches. However, the important issue of tumor resistance was often addressed by using either cell lines or transfected target cells (Bellucci et al., 2012; Khandelwal et al., 2015). Zhou et al. successfully discovered negative regulators of T-cell function in the tumor environment based on an in vivo pooled short hairpin RNA (shRNA) screen carried out in OT-I T-cells (P. Zhou et al., 2014).

Detailed analyses of CTL-killing efficiency are of high interest considering the large number of ongoing and upcoming studies on CTL modified for clinical use (i.e., with chimeric antigen receptor T (CAR-T) cells). As the CTL-killing efficiency is Ca^{2+} dependent, it is important to knockdown Ca^{2+} related proteins in primary human CTL by siRNAs.

This study aims to identify candidates that regulate Ca^{2+} dependent cytotoxicity. For this, genes showing differential expression between NK cells and CTL were intersected with members of known Ca^{2+}-signaling pathways and combined with putative key regulators. Subsequently, the effects of the candidate genes were tested after siRNA-silencing them in a real-time killing assay that is independent from the availability of blocking or activating agents.

2. Materials and methods

2.1. Ethical approval

The use of residual human material was approved by the local ethics committee (Ärztekammer des Saarlandes, reference 84/15, Prof. Dr. Rettig-Stürmer). Leukocyte reduction system chambers (LRSC), a byproduct of routine plateletpheresis from healthy donors, were kindly provided by the local blood bank in the Institute of Clinical Hemostaseology and Transfusion Medicine, Saarland University Medical Center. Blood donors provided written consent to use their blood for research purposes prior to samples being taken.

2.2. Reagents

Calcein-AM (#C3100) was purchased from ThermoFisher Scientific, staphylococcal enterotoxin A (SEA, #S9399), Infliximab (#Y0002047), ICI 118,551 hydrochloride (#127–5MG) and Maraviroc (#PZ0002) were from Sigma Aldrich. TRAM 34 (#2946) was purchased from R&D Systems and Venetoclax (ABT-199, #ab217298) from Abcam, Rituximab (lot oN7370B16) was from the local pharmacy (Universitätsklinikum Homburg, Hoffmann La Roche). All other chemicals and reagents not specifically mentioned were from Sigma Aldrich, ThermoFisher Scientific.

2.3. Preparation of human leukocytes, NK cells, un-stimulated CD8$^+$ T-cells and SEA-stimulated CD8$^+$ T-cells (SEA-CTL)

Human peripheral blood mononuclear cells (PBMC) were isolated from leukocyte reduction system chambers (LRSC) from TRIMA Accel systems after routine plateletpheresis of healthy donors at our local blood donation. Isolation of PBMC was carried out as described before (Knorck et al., 2018). Shortly, LRSC were rinsed with 8–10 ml Hank's balanced salt solution (HBSS, PAA, Cölbe, Germany) followed by a standard density gradient centrifugation (leukocyte separation medium LSM 1077, PromoCell, Heidelberg, Germany). After washing, remaining erythrocytes from the PBMC layer were lysed. The pellet was again washed in HBSS, and PBMC were counted (Z2 cell counter, Beckman and Colter). PBMC were stored at 4 °C until further use. Primary human NK cells and primary human un-stimulated CD8$^+$ T-cells were isolated from PBMC using Dynabeads Untouched™ Human CD8 T Cells (11349D, ThermoFisher Scientific) or Dynabeads Untouched™ Human NK Cells (11348D, ThermoFisher Scientific), respectively. These isolated cell populations were used for microarray analysis. To stimulate CD8$^+$ T-cells with *Staphylococcus aureus* enterotoxin A (SEA), 200–250 × 10^6 PBMCs were incubated in 1,6 ml AIMV medium supplemented with 10% FCS adding 0,8 μg SEA for 1 h (37 °C, 5% CO$_2$). Afterwards, cells were transferred into a 75 cm^2 cell culture flask containing 58 ml AIMV/10% FCS and 0.05 μg/ml IL-2. After 5 days, CD8$^+$ T-cells were isolated by using Dynabeads CD8 Positive isolation kit (11333D, Thermo Fisher Scientific) according to manufacturer's instructions except for the following: PBS/0.5% BSA (bovine serum albumin) without EDTA as buffer 1 and 18.75 μl instead of 25 μl Dynabeads CD8 for 1 ml PBMC (10^7 PBMC) were used. Isolated CD8$^+$ T-cells were cultured in complete AIMV medium with 0.05 μg/ml SEA added until further use and are referred to throughout this study as SEA-CTL.

2.4. Cells

Raji (ATCC CCL-86), T2 target cells and Epstein-Barr Virus-transformed B lymphoblastoid cell lines (EBV-LCLs) cells were cultured in RPMI-1640 (Thermo Fisher Scientific) supplemented with 10% FCS and 1% penicillin/streptomycin (#P433, Thermo Fisher Scientific) at 37 °C and 5% CO$_2$. MART (melanoma antigen recognized by T-cells) −1-specific CD8$^+$ T-cell clones (CTL-MART-1) were generated from an HLA-A2 positive donor and expanded as described previously (Friedmann et al., 2022). The MART-1-specific clone CTL-M3 from different expansions was used through the study (Friedmann et al., 2022).

2.5. Transfection of siRNA

Transfection of siRNA was carried out using the 4D Nucleofector (Lonza) following the manufacturer's instructions. For each transfection, 5–6 × 10^6 SEA-stimulated CTL (SEA-CTL) or MART-1 antigen-specific T-cell clones (CTL-MART-1) were washed in PBS/0.5%BSA and resuspended in 100 μl Nucleofector solution (Amaxa™ P3 Primary Cell 4D Nucleofector TM X Kit L, Lonza) with 4–6 μl of the appropriate siRNA (20–40 μM) added. Following nucleofection (program EO115), cells were cultured in AIMV/10% FCS for at least 6 h before adding 0.01 μg/

ml IL-2. SiRNAs were purchased from Dharmacon (a part of Horizon) and are listed in Table 1. Two different control siRNAs were used, control siRNA1 (non-targ#1) and control siRNA2 (non-targ#2) (Table 1).

2.6. Real-time killing assay

Cytotoxicity of siRNA-transfected SEA-CTL or CTL-MART-1 was measured with a real-time killing assay over a period of 4 h every 10 min (Kummerow et al., 2014). For each experiment, two different control populations were used. Thus, effector cells (SEA-CTL or CTL-MART-1) were transfected with control siRNA1 (non-targ#1) or control siRNA2 (non-targ#2) (Table 1). We used Raji or antigen (MART-1) pulsed T2 cells as target cells, respectively. Raji cells were pulsed with 1 μg/ml SEA in AIMV medium + 10% FCS for 30 min and T2 cells with 5 μg/ml MART-1 peptide. Subsequently, target cells were loaded with calcein-AM (500 nM, #C3100MP, Thermo Fisher Scientific) for 15 min, washed with AIMV medium without FCS and settled at a number of 2.5×10^4 cells per well into a 96-well black plate with clear bottom (#734–2480, VWR) for about 30 min. Next, transfected SEA-stimulated CTL or MART-1-T-cell clones were added to the corresponding target cells at the indicated effector to target ratio. Each condition was pipetted in duplicate. Target lysis was measured either with a Genios Pro (Tecan, Crailsheim, Germany) or with a Clariostar (BMG Labtech, Ortenberg, Germany) fluorescence plate reader using the bottom reading function at 37 °C. The real-time killing assay under Ca^{2+}-reduced conditions was performed as described in (X. Zhou et al., 2018). To study the impact of Maraviroc (20 mM stock solution in DMSO), Venetoclax (10 mM stock solution in DMSO), TRAM34 (10 mM stock solution in DMSO), Infliximab (35,6 mg/ml stock solution in dH_2O), or ICI 118,551 (10 mM stock solution in dH_2O) on cytotoxicity, SEA-CTL, or CTL-MART-1 were pre-incubated for 90 min in AIMV and 10 mM Hepes, with the indicated concentration of the corresponding inhibitor or as control the corresponding concentration of DMSO, or, in case of Infliximab, the corresponding concentration of IgG (Rituximab, 10 mg/ml stock solution). The killing assay was performed as described above. The indicated concentration of each inhibitor was present during the complete experiment.

2.7. RNA isolation and qRT-PCR

Experiments were done as described in (Wenning et al., 2011). Briefly, total RNA was isolated from either 1.5×10^6 SEA stimulated CTL or MART-1-specific $CD8^+$ T-cell clones using TRIzol reagent (Thermo Fisher Scientific) with 1 μl Glycogen (5 μg/μl, Thermo Fisher Scientific). 0.8 μg total RNA was used for reverse transcription and 0.5 μl of cDNA was used for quantitative real time polymerase chain reaction (qRT-PCR). qRT-PCR was carried out in a CFX96™ Real-Time System C1000™ Thermal Cycler (Software Biorad CFX Manager, Version 3.0) using QuantiTect SYBR Green PCR Kit (Qiagen, #204145). QuantiTect primer assays were purchased from Qiagen. Primer information is summarized in Table 2.

2.8. Data and statistical analysis

Data were tested for significance using Student t-test whenever Gaussian distribution was confirmed. Otherwise, the non-parametric Wilcoxon-Mann-Whitney test was used. Significance levels are as follows: $* p < 0.05$, $** p < 0.01$, $*** p < 0.001$, and ns refers to no significant difference. Data analyses were performed using Microsoft Excel 2016 and GraphPad Prism 7 software.

2.9. Microarray experiments

RNA was isolated from either 3×10^6 un-stimulated $CD8^+$ T-cells, approximately 1×10^6 SEA-stimulated CTL (SEA-CTL), or 3.0×10^6 NK cells. RNA processing, purity, and integrity of the input template RNA and microarray experiments were done as described before (Bhat et al., 2016). Microarray data are available at the GEO platform (https://www.ncbi.nlm.nih.gov/geo/) under the accession number GSE168692.

2.10. Microarray data pre-processing

The raw data were normalized using quantile normalization and log2 transformed with the statistical programming language R (Ihaka and Gentleman, 1996). Expression profiles of probe sets belonging to single genes were summarized/aggregated by computing the mean expression values as reported previously in (Hamed et al., 2015). Subsequently, data were subjected to differential expression analysis using the moderated t-test to identify the differentially expressed genes (DEGs) between the various sample groups. Namely, genes that exhibited 2-fold changes and p-value below a cutoff of 0.05 were classified as differentially expressed genes (DEGs). P-values were adjusted using the Benjamini-Hochberg (Hochberg and Benjamini, 1990) procedure to limit the false discovery rate to 5%.

2.11. Identification of candidate genes

Candidate genes that are possibly responsible for modulating the killing efficiency of SEA-CTL are assumed to show differential expression between SEA-CTL ($CD8^+$ SEA) and NK samples. These are termed SEA-DEGs (differentially expressed genes). From this list, we deleted

Table 1

siRNAs used in this study: Perforin siRNA was synthesized by Microsynth sense 5′ OMeA-OMeA (AGAUUGGAUACGCAU)₁₅ d(CAG) dOMeA-dOMeT-dOMeT 3′; antisense 3′ OMeT-OMeT-UCUAACCUAUGCGUAGUC-dU 5′. Each gene listed in the table was targeted by a pool of four individual siRNAs.

gene	gene accession number	Dharmacon, SmartPool order number	gene	gene accession number	Dharmacon, SmartPool order number
RPLP0	NM_001002	L-010864–00	DMPK	NM_004409	L-004637–00
RGS10	NM_002925	L-008472–02	BRCA1	NM_007298	L-003461–00
CCR5	NM_000579	L-004855–00	EGR1	NM_001964	L-006526–00
HPRT1	NM_000194	L-008735–00	EGR2	NM_000399	L-006527–00
ADCY3	NM_004036	L-006799–00	LAT2	NM_014146	L-013570–02
PKIA	NM_181839	L-012321–00	KCNN4	NM_002250	L-004461–00
TNF	NM_000594	L-010546–00	BCL2	NM_000657	L-003307–00
PRKAR1B	NM_001164759	L-030847–02	RCAN3	NM_013441	L-020467–02
ADRB2	NM_000024	L-005426–01	FASLG	NM_000639	L-011130–00
NOS3	NM_006490	L-006490–00	CALML3	NM_005185	L-019122–02
IFNG	NM_000619	L-019379–00	CAMK4	NM_001744	L-004944–00
CD40LG	NM_000074	L-011006–00	DMTN	NM_001114139	L-003663–02
SGK1	NM_005627	L-003027–00	PLCG2	NM_002661	L-008339–02
POU2AF1	NM_006235	L-020133–00	NMUR1	NM_006056	L-005590–00
ANO9	NM_001012302	L-026726–02	non-targ#1	no accession number	D-001210–01
AHR	NM_001621	L-004990–00	non-targ#2	no accession number	D-001210–02
F2R	NM_001992	L-005094–00			

Table 2

Primers used in this study. Primers for the reference genes RNAPol (NM_000937) and TBP (NM_003194) are taken from (Wenning et al., 2011) and primers for perforin (NM_005041 and NM_001083116) from (Bhat et al., 2016). Primers for FASLG (NM_000639) forward 5′ GCACACAGCATCATCTTTGG 3′ and reverse 5′ CAA-GATTGACCCCGGAAGTA 3′.

gene		QuantiTect Primer Assay	gene		QuantiTect Primer Assay
ADCY3	Hs_ADCY3_1_SG	QT00075348	IFNG	Hs_IFNG_1_SG	QT00000525
ADRB2	Hs_ADRB2_1_SG	QT00200011	KCNN4	Hs_KCNN4_1_SG	QT00003780
AHR	Hs_AHR_2_SG	QT02422938	LAT2	Hs_LAT2_1_SG	QT00010934
ANO9	Hs_ANO9_1_SG	QT01322643	NFAT5	Hs_NFAT5_1_SG	QT00049210
BCL2	Hs_BCL2_1_SG	QT00025011	NMUR1	Hs_NMUR1_1_SG	QT00080311
BRCA1	Hs_BRCA1_1_SG	QT00039305	NOS3	Hs_NOS3_1_SG	QT00089033
CALML3	Hs_CALML3_1_SG	QT00214935	PAK1	Hs_PAK1_1_SG	QT00068306
CAMK4	Hs_CAMK4_1_SG	QT00038101	PKIA	Hs_PKIA_2_SG	QT02289658
CATSPER1	Hs_CATSPER1_1_SG	QT00027965	PLCG2	Hs_PLCG2_1_SG	QT00050393
CCR5	Hs_CCR5_1_SG	QT00998802	POU2AF1	Hs_POU2AF1_1_SG	QT00001540
CD40LG	Hs_CD40LG_1_SG	QT00000343	PRKAR1B	Hs_PRKAR1B_2_SG	QT02306521
DMPK	Hs_DMPK_1_SG	QT00094199	RCAN3	Hs_RCAN3_1_SG	QT00075369
DMTN	Hs_DMTN_1_SG	QT00493052	RGS10	Hs_RGS10_1_SG	QT00235900
Egr1	Hs_EGR1_1_SG	QT00218505	RPLP0	Hs_RPLP0_1_SG	QT00075012
Egr2	Hs_EGR2_1_SG	QT00000924	SGK1	Hs_SGK1_1_SG	QT00041293
F2R	Hs_F2R_1_SG	QT00230489	TNFa	Hs_TNF_1_SG	QT00029162
HPRT1	Hs_HPRT1_1_SG	QT00059066			

genes that are also differentially expressed between "SEA"-stimulated cells and "un"-stimulated cells. This yielded 2349 SEA-DEGs between CD8$^+$ SEA and NK samples. We then used two strategies for pruning this set of differentially expressed genes to a manageable number of candidate genes.

A list of 512 calcium-associated genes was compiled from the KEGG (Kyoto Encyclopedia of Genes and Genomes) pathway (Kanehisa et al., 2016), the Gene Ontology (The Gene Ontology, C., 2019), the Wiki-pathways (Martens et al., 2020), and the PathwaysFinder (Yao et al., 2004) databases.

Strategy 1: The list of 2349 SEA-DEGs was intersected with the 512 "Ca^{2+}-associated genes" and this resulted in 61 Ca^{2+}-associated DEGs. From this list we removed genes having low expression levels in SEA-CTL ($2^{7.2}$ (fluorescence value < 147), the mean expression value). After this, 29 candidate genes remained.

Strategy 2: This strategy followed that of our method TopControl (Nazarieh and Helms, 2019). First, the set of 2349 SEA-DEGs was provided as input to the webserver TFmiR (Hamed et al., 2015). TFmiR constructed a differential co-regulatory network involving 98 genes (transcription factors or target genes) and identified the set of 10% most connected hub genes. In this network, we identified a minimum dominating set (MDS) of genes using the instruction level parallelism (ILP) approach. In the largest connected component underlying the undirected graph of this network, we identified a minimum connected dominating set (MCDS) using the heuristic approach. Both algorithms are described in (Nazarieh et al., 2016). 47 genes belonged to at least one of these three sets (hubs, MDS, MCDS). Intersecting this set of 47 genes with the 512 "calcium-associated genes" gave 7 candidate genes. Of these 7 candidates, the gene ATF3 was excluded due to its low expression level in SEA-CTL, and four other genes: BCL2, TNF, FASLG, and EGR1 were identified by both strategies.

The combination of both strategies gave 31 unique candidate genes that were further investigated.

3. Results

3.1. Different bioinformatic strategies identify 31 candidates with a potential impact on the regulation of Ca^{2+}-dependent killing mechanism

Lytic granule (LG)-dependent cytotoxicity of CTL (cytotoxic T lymphocytes) and NK cells depends on Ca^{2+} influx through STIM-activated Orai channels (Maul-Pavicic et al., 2011; X. Zhou et al., 2018). Although CTL and NK cells use similar mechanisms to kill their respective targets, the Ca^{2+} dependence of their cytotoxic efficacy is slightly different (X. Zhou et al., 2018). Since it is known for CTL and NK cells that STIM and

Orai are the main players for Ca^{2+}-dependent cytotoxicity, we are interested in identifying proteins besides them that have an additional impact on the regulation of Ca^{2+}-dependent killing mechanisms. In the following, these molecules will be termed "candidates". To this end, we performed expression analysis based on microarray technology of the following primary human cell populations: 1. *Staphylococcus aureus* enterotoxin A (SEA) stimulated CD8$^+$ T-cells (SEA-CTL, n = 11), 2. NK cells (n = 11) and as a control population 3. un-stimulated CD8$^+$ T-cells which are not yet killing competent (purified from human PBMC without any additional cell cultivation, n = 11). Expression data from microarray were background corrected and expression data lower than $2^{7.2}$ (fluorescence value < 147) were considered as too low or not expressed as confirmed for a number of genes by quantitative RT-PCR.

Candidates were identified by two independent bioinformatic strategies. The first strategy revealed 2349 differentially expressed genes (DEG) among NK cells and SEA-CTL from the microarray data. Besides, we identified 512 genes in Ca^{2+}-signaling pathways of different databases (for details see Material and Methods). Intersection of these two gene sets resulted in 86 candidates. Among these 86 candidates, we excluded those which were also differentially expressed between SEA-CTL and un-stimulated CD8$^+$ T-cells assuming that these genes have been regulated due to stimulation by SEA. Thereby, 25 genes were eliminated from the 86 candidates. Among the remaining 61 genes, only 29 were reasonably high expressed in SEA-CTL. Thus, this first strategy led to 29 candidates potentially regulating Ca^{2+} dependent CTL cytotoxicity (Fig. 1A).

In a second strategy, using the prioritization approach TopControl (Nazarieh and Helms, 2019), we prioritized another set of candidates based on a gene-regulatory network of the 2263 DEGs between SEA-CTL and NK cells that was constructed with the TFmiR webserver (Hamed et al., 2015). As candidates, we considered hub genes and dominating genes of the regulatory network (see methods). This strategy identified 7 candidates ((Nazarieh and Helms, 2019), Fig. 1B). Of these 7 candidates, ATF3 was too low expressed in SEA-CTL, and 4 further candidate genes (BCL2, TNF, FASLG, and EGR1) overlapped with those identified by the first strategy (Fig. 1B, labeled in red, Supplementary Figure 1). Combining the candidates from both analyses led to 31 potential candidates.

3.2. Down-regulation of 10 randomly selected candidates suggests a possible impact of KCNN4 and BCL2 on the cytotoxicity of SEA-CTL

Before analyzing all 31 candidates, we randomly selected 10 candidates (Fig. 1C) to establish our experimental set-up. First, we tested which of the candidates modulate the cytotoxic efficiency in SEA-CTL by
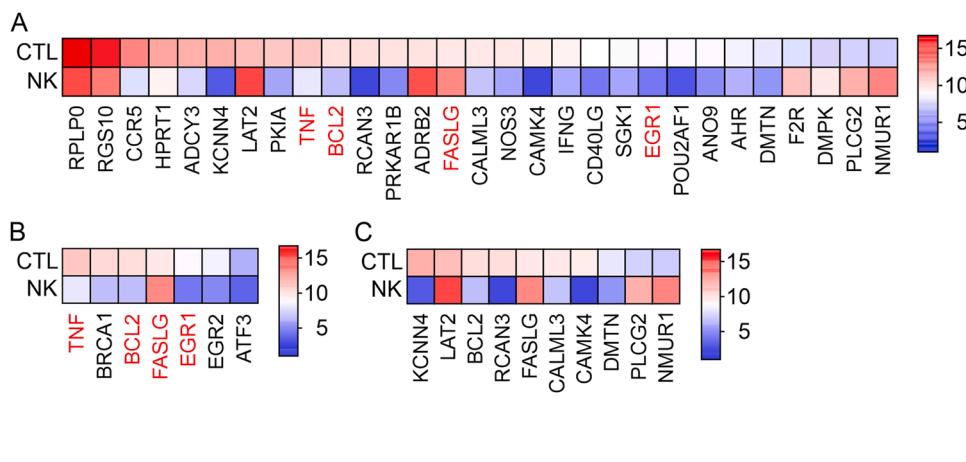
Fig. 1. Heatmap representing the expression levels of candidates in SEA-stimulated CD8$^+$ T-cells (CTL) and NK cells (NK) identified by bioinformatic strategy 1 and 2. (A) Expression levels of 29 candidate genes with reasonably high expression in SEA-CTL identified by strategy 1 and analyzed in the following in SEA-CTL. (B) Expression level of the 7 candidate genes identified by strategy 2 and representing Ca^{2+}-associated top control genes. Genes labeled in red were identified by both strategies (A,B). C. Candidates randomly selected from all candidates in order to establish our experimental screening strategy in SEA-CTL. The color scale bars show the corresponding normalized expression values. Blue color indicates low expression whereas red color indicates high expression.
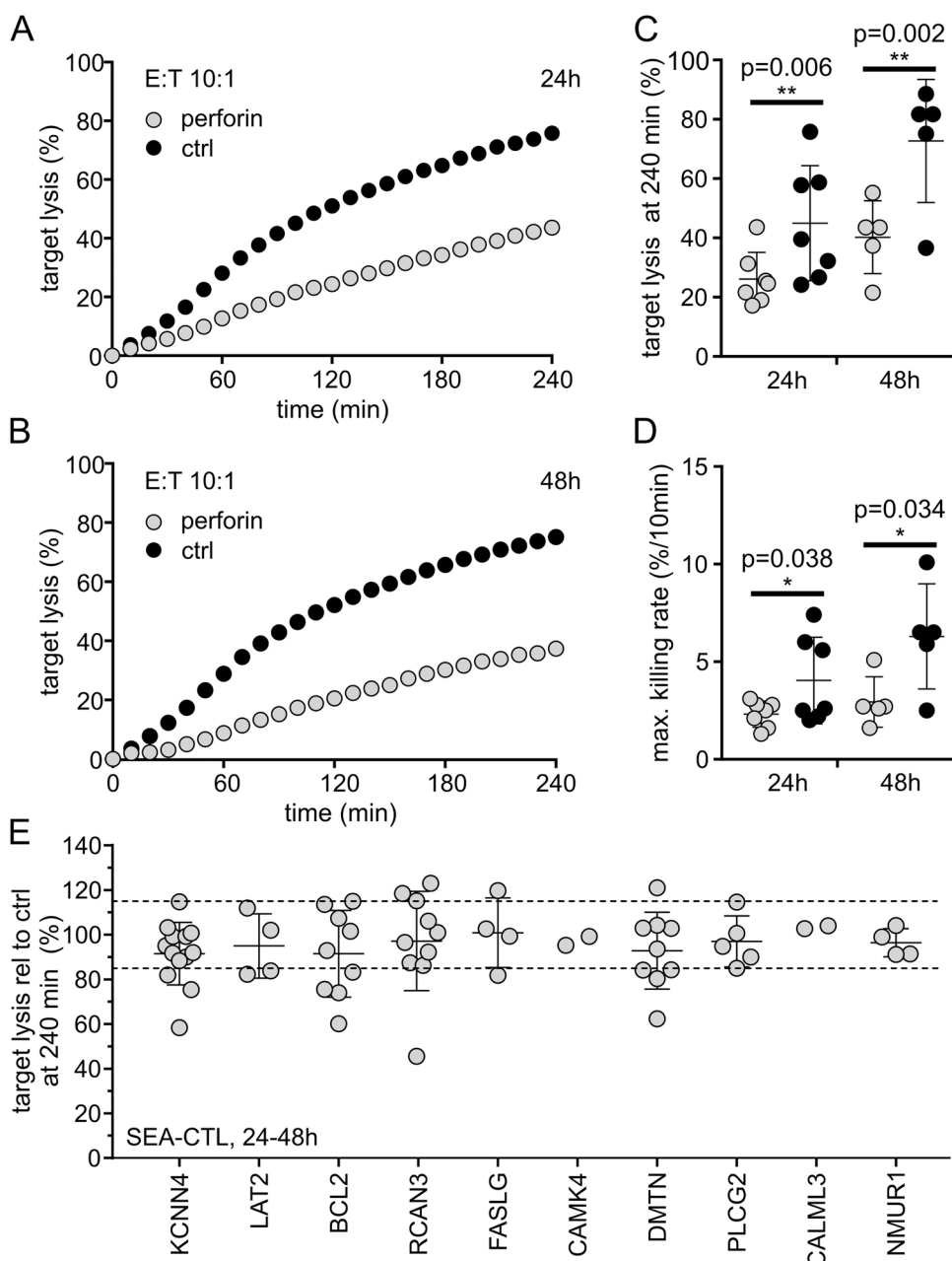
Fig. 2. Real-time killing assay of SEA-stimulated CTL (SEA-CTL) as effector cells and SEA-pulsed Raji cells as target cells with an effector to target ratio (E:T) of 10:1 or 20:1. A–D. Real-time killing assay with perforin siRNA transfected SEA-CTL (gray) or the mean of two different control siRNAs (black). A, B. Representative killing traces at 24 h (A) and 48 h (B) after transfection. C, D. Statistical analysis of endpoint lysis after 240 min (C) and maximal killing rates (D), n = 7 (24 h after transfection) and n = 5 (48 h after transfection). E. Endpoint target lysis of SEA-CTL transfected with siRNAs against 10, randomly chosen candidates (compare Fig. 1 C) relative to the mean of SEA-CTL transfected with two different control siRNAs (24 h and 48 h after transfection in AIMV medium). Data are shown as mean + /- SD from 2 to 10 different donors. KCNN4, n = 10; LAT2, n = 4; BCL2, n = 6; RCAN3, n = 5; FASLG, n = 4; CAMK4, n = 2; DMTN, n = 9; PLCG2, n = 5; CALML3, n = 2; NMUR1, n = 4.

down-regulating candidate expression levels via siRNA and a subsequent real-time killing assay (Kummerow et al., 2014). As positive control, we transfected an siRNA against perforin which reduced the cytotoxic efficiency as expected (Fig. 2A-D, (X. Zhou et al., 2018)). Next, we transfected the SEA-CTL with a pool of four individual siRNAs directed against each candidate (Table 1) and analyzed these cells 24 and 48 h after transfection by the real-time killing assay with SEA-loaded Raji cells as targets (Fig. 2E). As control conditions, we routinely used SEA-CTL that were each transfected with two different control siRNAs (Table 1). All results are always normalized relative to these two controls. The killing efficiency in the perforin siRNA transfected SEA-CTL was reduced by about 42% after 24 h (perforin mean 26.1% +/- 3.4% SEM and ctrl mean 45.0% +/- 7.3% SEM) and by about 45% after 48 h (perforin mean 40.2% +/- 5.5% SEM and ctrl mean 72.7% +/- 9.3% SEM) as shown in representative killing traces (Fig. 2A, B) and the endpoint target lysis analyzed in 5–7 different donors (Fig. 2C). Furthermore, the maximal killing rates (highest target lysis between two measurement points (%/10 min)) confirmed that a stronger effect exists 48 h after transfection (Figs. 2D, 42.5% after 24 h, 51.7% after 48 h, reduction compared to control conditions). When we explored the influence of the randomly selected candidates on the killing efficiency, no significant difference to control siRNA transfected SEA-CTL was detected within the sensitivity limit of the killing assay (target lysis at 240 min should be either lower than 85% or higher than 115% compared to the mean of control transfected siRNA (normalized to 100%), Fig. 2E). Downregulation of several candidates such as KCNN4, BCL2 and DMTN showed a tendency towards a reduced killing efficiency (KCNN4 91.5% relative to ctrl +/- 3.9% SEM, BCL2 91.5% relative to ctrl +/- 6.5% SEM and DMTN 92.2% relative to ctrl +/- 5.7% SEM), but the variability between different experiments and between different blood donors was too large to reach statistical significance.

3.3. Using Mart-1 specific T cell clones (CTL-MART-1) reduces SEA-CTL`s donor variability and improves the efficiency of siRNA downregulation

Since the observed variability in the killing efficiency of SEA-CTL might unfavorably compromise the interpretation of the results of our initial screen, we implemented another strategy to stimulate CTL. To this end, we used MART-1-specific CTL clones from primary human PBMC (CTL-MART-1, recently established in our lab (Friedmann et al., 2022)) and compared the variance in target lysis of CTL-MART-1 to SEA-CTL transfected with control siRNA in the real-time killing assay.

Reassuringly, the target lysis at 240 min, analyzed at days 1 and 2 after transfection, was much more stable in CTL-MART-1 than in SEA-CTL (Fig. 3A). The cytotoxic efficiency was higher in CTL-MART-1 but most importantly the standard deviation was much lower: Mean and standard deviations of the target lysis after 240 min for MART-1-CTL were 64.0 + /- 14.1% (day1) and 68.3 + /- 10.9% (day2) compared to 36.3% + /- 19.7% (day1) and 53.3% + /- 31.2% (day2) for SEA-CTL. The higher variation of SEA-CTL likely results from blood donor variability. In addition to the lower variation of CTL-MART-1, we also found that siRNA down-regulation was more effective in CTL-MART-1 compared to SEA-CTL as tested for 8 candidates (Fig. 3B). This was true for all candidates except for BCL-2. Finally, we found the expression of 35 genes (Table 2, except NOS3 due to lack expression in CTL-MART-1) moderately positively correlated in CTL-MART-1 and SEA-CTL (Fig. 3C).

Based on the lower variability, the overall better efficiency of downregulation by siRNA and moderate correlation of gene expression, we switched from SEA-CTL to CTL-MART-1 as effector cells to screen potential candidates for their impact on target cell killing. As a positive control, we used again siRNA against perforin (compare Fig. 2) and analyzed transfected CTL-MART-1 by the real-time killing assay with MART-1-peptide loaded T2 cells as target cells (Fig. 4A-C). Cytotoxicity was again reduced by the down-regulation of perforin (Fig. 4A), however the effect was not as prominent as for SEA-CTL (compare Fig. 2). The effect on the maximal killing rate was stronger compared to the effect on the endpoint target lysis (Fig. 4B,C) what suggests a stronger effect in the early phase (first hour) of the killing assay. Since the down-regulation efficiency is a critical point for the screening project, we first explored the down-regulation efficiency in CTL-MART-1 for all candidates (except NMUR1 which was only expressed at very low levels). Expression of each gene was normalized to the mean of two control siRNAs transfected into CTL-MART-1. Since the down-regulation efficiency was variable for different target genes (Fig. 4D), we only tested those candidates when the mRNA level of the corresponding candidate was at most 55% of the level in control conditions (24–30 h after transfection). Consequently, we excluded TNFa, BCL2, ADRB2, CALML3, IFNG, EGR1, DMPK, and EGR2 (compare Fig. 4D, upper dotted line). Except these genes, the siRNAs against all other candidates were transfected into CTL-MART-1 and analyzed by the real-time killing assay. A summary of the target cell lysis, 24–48 h after transfection, is presented in Fig. 4E. Again, none of the candidates showed an average target lysis at 240 min higher than 115% or lower than 85%.
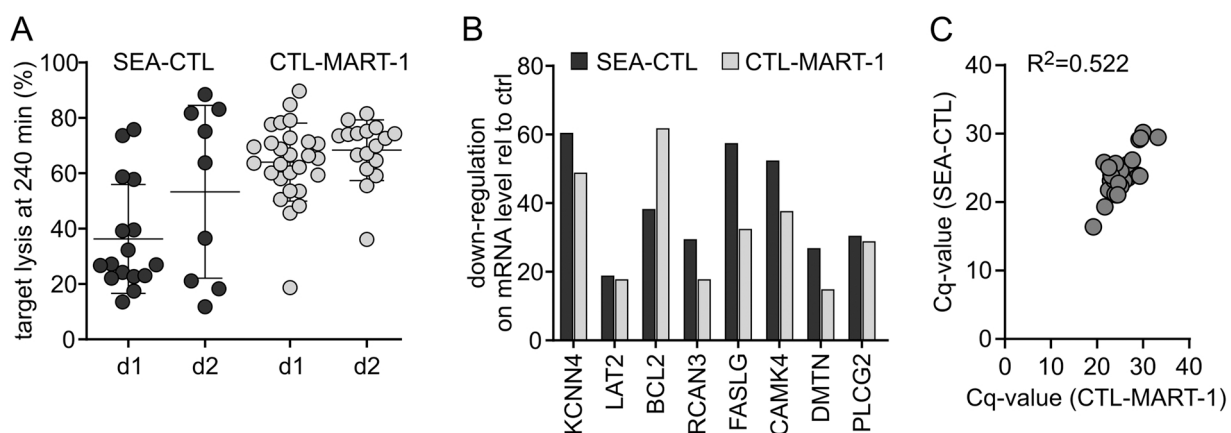

Fig. 3. A. Endpoint target lysis of SEA-stimulated CTL (SEA-CTL, black) in comparison to MART-1 specific CTL (CTL-MART-1, gray) one day (d1) or two days (d2) after transfection with control siRNAs. Data points correspond to the mean of two different control siRNAs. Bars show the mean + /- SEM, SEA-CTL d1 n = 16, d2 n = 9; CTL-MART-1 d1 n = 20, d2 n = 17. B. Relative mRNA expression of 8 selected candidates 24–30 h after transfection of SEA-CTL (black; n = 3 for KCNN4; n = 4 for BCL2, all other candidates n = 1) or CTL-MART-1 (gray; n = 3 for KCNN4 and BCL2; n = 2 for LAT2; all other candidates n = 1) with the corresponding siRNA. The expression level of mRNA in control siRNA transfected SEA-CTL was set to 100%. C. Expression of 35 genes (Table 2) analyzed by qRT-PCR in SEA-CTL (pool of 3 donors) and CTL-MART-1.
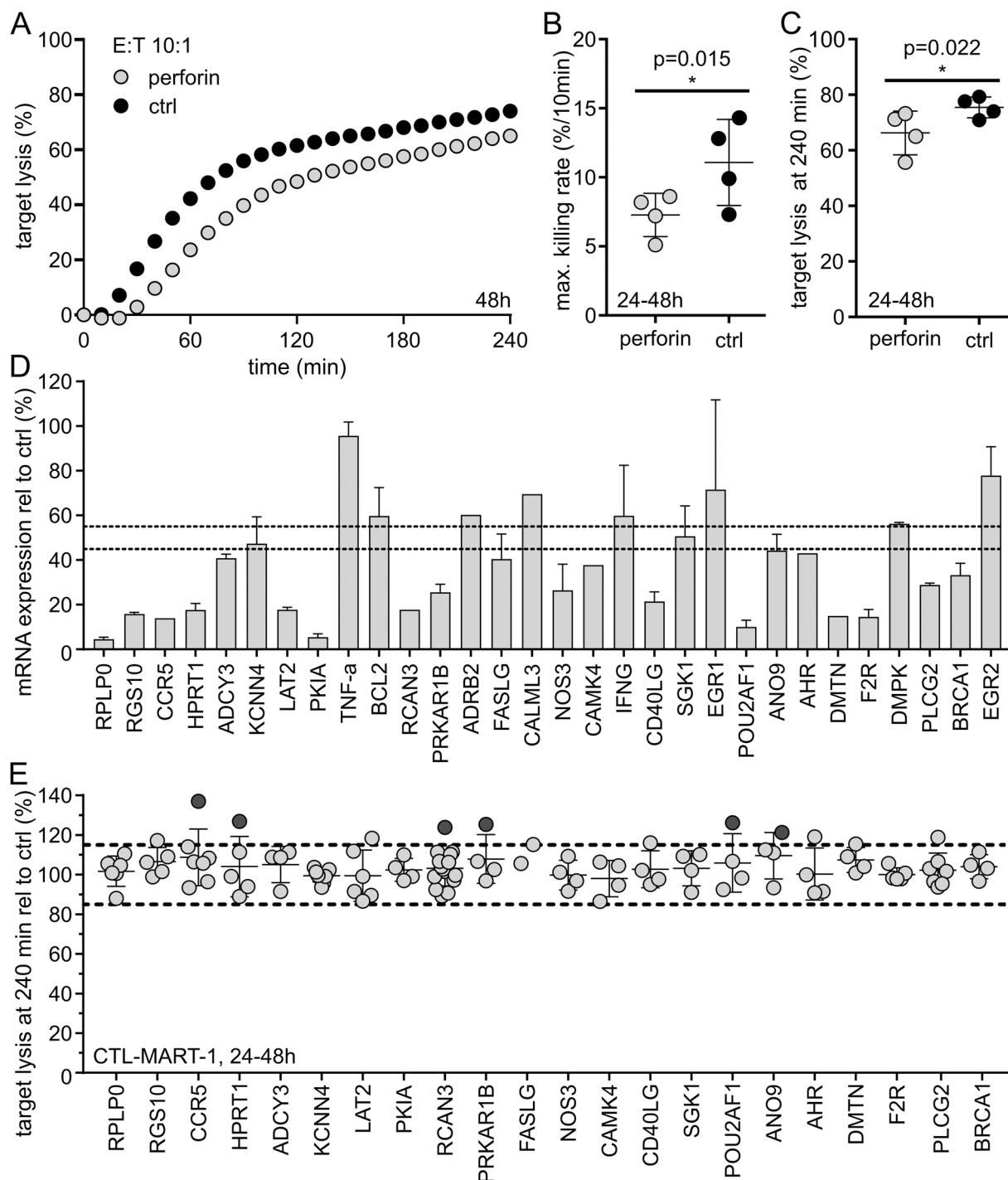
Fig. 4. A-C. Real-time killing assay of perforin down-regulated MART-1 specific CTL (gray, CTL-MART-1) in comparison to control siRNA (mean of two control siRNAs) transfected CTL-MART-1 (black, ctrl). As target cells, MART-1 loaded T2 cells were used with an effector to target ratio (E:T) of 5:1 or 10:1. A. Representative killing traces 48 h after transfection. Statistical analysis of the maximum killing rate 24 h and 48 h after transfection (number of transfections, n = 2, B) and the endpoint target lysis 24 h and 48 h after transfection (number of transfections, n = 2, C). Data are shown as mean +/- SD. D. Relative mRNA expression of all tested candidates 24–30 h after transfection of CTL-MART-1 with the corresponding siRNAs (CCR5, ADRB2, AHR, RCAN3, CALML3, CAMK4, DMTN, n = 1; KCNN4, BCL2, n = 3; all other candidates, n = 2, partially shown in Fig. 3B for CTL-MART1). The mRNA expression level in control siRNA transfected CTL-MART-1 was set to 100%. E. Endpoint target lysis of CTL-MART-1 transfected with siRNA against selected candidates relative to the mean of CTL-MART-1 transfected with two different control siRNAs. MART-1 loaded T2 cells were used as target cells with an E:T ratio of 5:1 or 2:1. Data are from 2 to 11 different transfections (n = 2 for ADCY3, PKIA, PRKAR1B, FASLG, NOS3, CAMK4, CD40LG, SGK1, POU2AF1, ANO9, AHR, DMTN, DMPK and BRCA1; n = 3 for RPLP0, RGS10, LAT2 and F2R; n = 4 for CCR5 and PLCG2; n = 6 for KCNN4; n = 11 for RCAN3). Values higher than 120% target lysis at 240 min compared to the control siRNAs are labeled in dark gray. Data are shown as mean +/- SD.

3.4. Down-regulation of KCNN4 and RCAN3 results in altered cytotoxicity under Ca^{2+}-limiting conditions

Since Orai and STIM proteins are the key molecular players for Ca^{2+}-entry in CTL, we reasoned that it may be difficult to identify further candidates regulating Ca^{2+}-dependent cytotoxicity without putting a selective pressure on the system. Thus, in a next step, we tested several candidates under Ca^{2+}-limiting conditions in CTL-MART-1 (by adding EGTA to the medium during the real-time killing assay, (X. Zhou et al., 2018)) based on different arguments. 1. KCNN4 and SGK1 were selected since they showed an intermediate level knockdown of target mRNAs between 45% and 55% relative to control conditions (Fig. 4D). In cases of incomplete or intermediate downregulation, one can easily overlook an effect due to the low efficiency of siRNA down-regulation. 2. Candidates which showed a target cell lysis of either less than 80% or more than 120% at least in one single experiment. This criterion led to the selection of CCR5, HPRT1, RCAN3, PRKAR1B, POU2AF1 and ANO9 (Fig. 4E, dark gray dots). Altogether, eight out of the originally 31 candidates were tested in a real-time killing assay under Ca^{2+}-limiting conditions. To reduce the extracellular Ca^{2+} concentration ($[Ca^{2+}]_{ext}$), various concentrations of EGTA were added to the medium during the real-time killing assay. The addition of 0.80 up to 0.95 mM EGTA leads to a $[Ca^{2+}]_{ext}$ of about 10–150 μM (X. Zhou et al., 2018). Considering experiment-to-experiment variability that was observed even for CTL-MART-1 (Fig. 3A), we applied different EGTA concentrations in different experiments. To enable regulation of Ca^{2+}-dependent cytotoxicity to take place in both directions (enhancement or reduction), we aimed at an intermediate cytotoxic efficiency under Ca^{2+}-limiting conditions. Therefore, we always optimized the EGTA concentrations for each experiment to reach a cytotoxic efficiency between 30%−85% under Ca^{2+}-limiting conditions relative to control conditions. Fig. 5A shows examples of killing traces for control siRNA transfected CTL-MART-1 and for MART-1 peptide-loaded T2 cells as target cells with different EGTA concentrations. From these different traces, the appropriate condition was determined to be 0.93 mM EGTA because this yielded a cytotoxicity in the desired range. Choosing such a cytotoxicity range should facilitate the detection of effects of the different candidates.

Based on these considerations, we tested the eight candidates according to the criteria mentioned above with the real-time killing assay under Ca^{2+}-limiting conditions. As an example, Fig. 5B illustrates killing traces of KCNN4 down-regulated MART-1-CTL versus control siRNA transfected cells in the defined killing range. Down-regulation of KCNN4 significantly reduced the killing capacity of MART-1-CTL by about 70% (mean target lysis at 240 min 31.2% +/- 14.5% SEM) whereas down-regulation of RCAN3 enhanced the killing capacity of MART-1-CTL (mean target lysis at 240 min 119.7% +/- 17.0% SEM) (Fig. 5C). If the lowest "outlier" point is omitted from the analysis, the enhancement by RCAN3 down-regulation is significant (p = 0.026). When we separated the assembled data for CTL-MART-1 (Fig. 4E) into the two different time points, day 1 and day 2 after transfection, down-regulation of RCAN3 was significant at day 2 even without the addition of EGTA (Supplementary Figure 2). Downregulation of none of the other 6 candidates revealed any significant effects, only downregulation of CCR5 led to high variations in killing efficiency at 240 min, a tendency which was already visible without limiting the $[Ca^{2+}]_{ext}$ (Fig. 4E, Fig. 5C).

3.5. Inhibition of KCNN4, BCL2 and CCR5 results in altered cytotoxicity under non-altered Ca^{2+}-conditions

Transfection with siRNA always comes at the risk of an insufficient target mRNA down-regulation (compare Fig. 4D). Therefore, we also implemented an alternative approach to test for a potential function of the candidates. For 5 of our candidates, inhibitory substances are available. We tested TRAM34 on KCNN4 to confirm the down-regulation in the killing efficiency seen in CTL-MART-1. Infliximab was used against TNFα, ICI118.551 against ADRB2, Maraviroc against CCR5 and Venetoclax against BCL2. The latter four ones were targeted because mRNA down-regulation of the respective mRNA was insufficient or the killing efficiency very variable (compare Fig. 4D,E).

CCR5 inhibition by 10 μM Maraviroc had a slightly reducing (but significant) impact on target cell lysis (Maraviroc mean 74.2% +/- 8.9% SEM and DMSO control mean 82.3% +/- 8.0% SEM) (Fig. 6A). 50 μM of the KCNN4 inhibitor TRAM34 reduced the target cell efficiency in CTL-MART-1 by about 40% (TRAM34 mean 47.7% +/−4.8% SEM and DMSO control mean 75.2% +/- 6.7% SEM) (Fig. 6B). The same tendency was also found in SEA-CTL, but this was not significant (Fig. 6B). Next, we tested the inhibitors against the three candidates with insufficient mRNA down-regulation. The application of the TNFα inhibitor Infliximab had no impact on the killing capacity of CTL-MART-1, neither with 1 μg/ml nor with 10 μg/ml antibody in comparison to control conditions
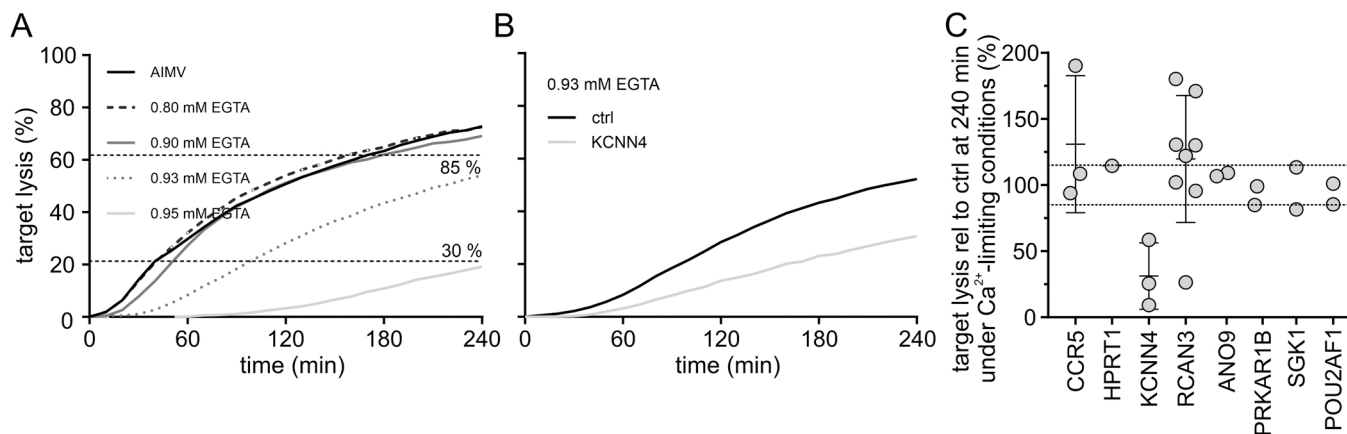
Fig. 5. : Real-time killing assay under Ca^{2+}-limiting conditions manipulated by the addition of EGTA using CTL-MART-1 as effector and MART-1 peptide loaded T2 cells as target cells with an E:T ratio of 2:1. A. Representative killing traces of CTL-MART-1 transfected with a control siRNA using different concentrations of EGTA to determine the extracellular calcium concentration leading to a 30–85% reduction in killing capacity after 240 min relative to control (defined as Ca^{2+}-limiting condition). B. Representative killing traces of CTL MART-1 transfected with control siRNA (mean of two control siRNAs, black) or with KCNN4 siRNA (gray) under Ca^{2+}-limiting conditions (0.93 mM EGTA) 24 h after transfection. C. Endpoint target lysis of CTL-MART-1 transfected with siRNA against selected candidates relative to the mean of CTL-MART-1 transfected with two different control siRNAs. Each killing assay was performed under Ca^{2+}-limiting conditions (see Fig. 5 A) 24–48 h after transfection. Data are from 1 to 6 different transfections of CTL-MART-1 (HPRT1, ANO9, PRKAR1B, SGK1 and POU2AF1, n = 1; KCNN4 and CCR5, n = 2; RCAN3, n = 6) with 1 or 2 data points (24 h and 48 h after transfection). Data are shown as mean + /- SD.
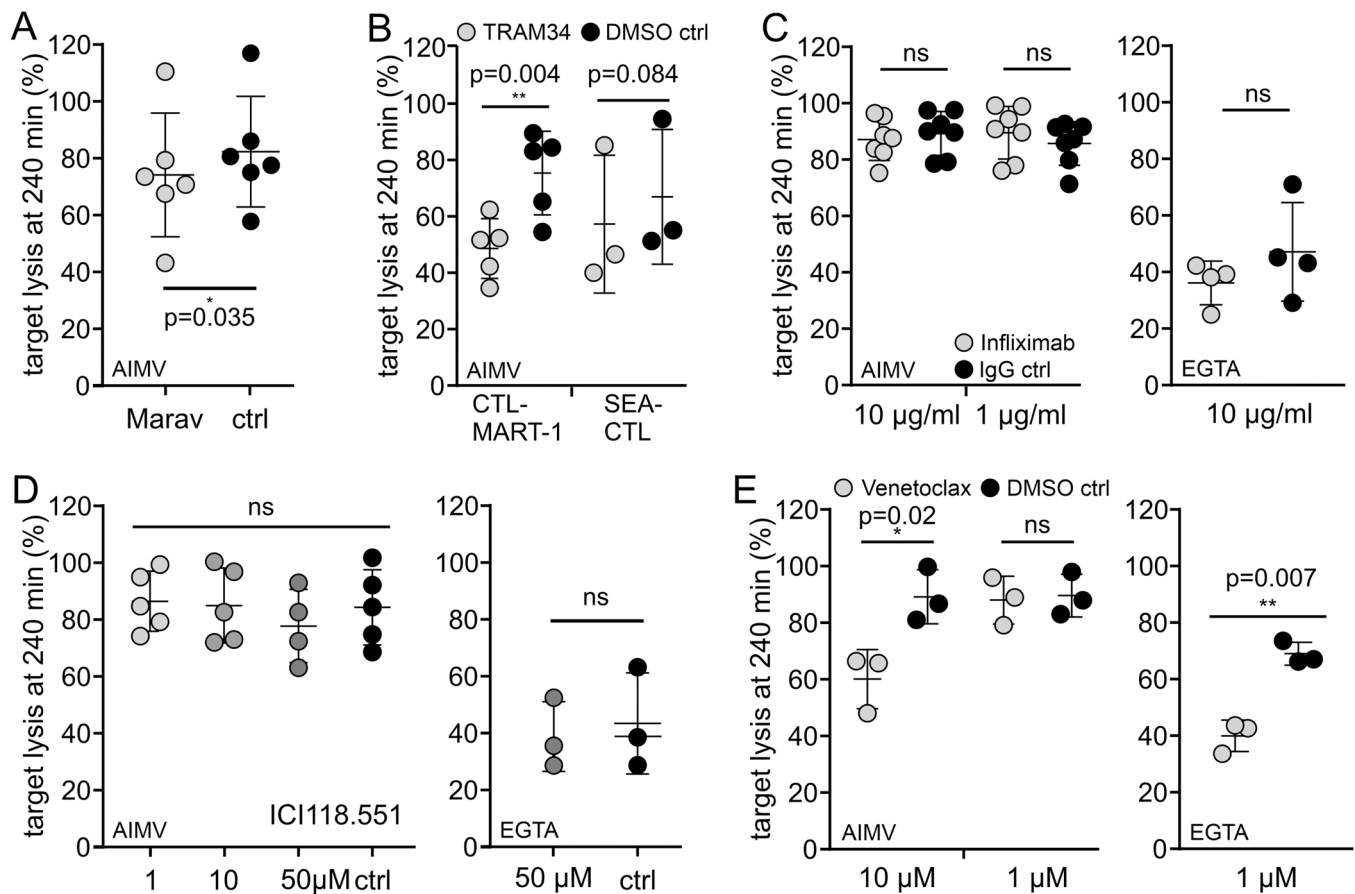
Fig. 6. Real-time killing assay with various inhibitory substances using CTL-MART-1 as effector and MART-1 peptide loaded T2 cells as target cells with an E:T ratio of 2:1. A. Target lysis after 240 min with the application of 10 μM Maraviroc (Marav, gray circles) to inhibit CCR5 and DMSO as control (crtl, black circles). B. Target lysis after 240 min with the application of 50 μM TRAM34 (gray circles), an inhibitory substance of KCNN4, and DMSO as vehicle control (black circles). Right panel, SEA-CTL were used as effector and SEA-loaded Raji cells as target cells with an E:T ratio of 10:1. C. Target lysis after 240 min using Infliximab (gray circles), an inhibitory antibody of TNFa either in AIMV (left) or under Ca^{2+}-limiting conditions (right). Rituximab was used as IgG control (black circles) in the same concentration used for Infliximab. D. Target lysis after 240 min with the application of ICI 118,551 (gray circles), inhibiting ADRB2 with different concentrations. Killing assay was performed in AIMV (left) or under Ca^{2+} -limiting conditions (right). E. Target lysis after 240 min in the presence of 1 or 10 μM Venetoclax (gray circles) to inhibit the function of BCL2 in AIMV (left) and under Ca^{2+}-limiting conditions manipulated by the addition of EGTA (right). Data are from 3 to 7 different experiments with CTL-MART-1 or from 3 different donors (SEA-CTL, B). Data are shown as mean + /- SD.

with Rituximab, an IgG anti-CD20 antibody, (Fig. 6C, left panel). When EGTA was added to the real-time killing assay to induce Ca^{2+}-limiting conditions, a slight tendency towards an impairment of the killing capacity of CTL-MART-1 was detected (Fig. 6C, right panel). Similarly, the application of ADRB2 inhibitor ICI 118,551 revealed only a non-significant tendency when using a high concentration of 50 μM independent of the use of Ca^{2+}-limiting or non-limiting conditions (Fig. 6D). The last candidate, BCL2, is inhibited by Venetoclax. In standard conditions (normal medium, AIMV, 800 μM $[Ca^{2+}]_{ext}$), 10 μM Venetoclax inhibited the target lysis at 240 min by about 33% (Venetoclax mean 60.1% +/−6.0% SEM and DMSO control mean 89.2% +/- 5.5% SEM), but not at 1 μM. (Fig. 6E, left panel). However, application of 1 μM Venetoclax had a highly significant impact on the killing efficiency of CTL-MART-1 under Ca^{2+}-limiting conditions (Venetoclax mean 40.0% +/−3.2% SEM and DMSO control mean 69.0% +/- 2.3% SEM, Fig. 6E) suggesting that Ca^{2+}-limiting conditions unveil the effect of BCL2 on Ca^{2+}-homeostasis.

In summary, out of 31 potential candidates that we tested, we identified four hits, namely the proteins CCR5, KCNN4, RCAN3 and BCL2 that clearly affect the efficiency of Ca^{2+}-dependent cytotoxicity of CTL-MART-1. Notably, the inhibition of CCR5, BCL2 and KCNN4 decreased cytotoxicity whereas the down-regulation of RCAN3 increased the cytotoxicity.

4. Discussion

Ca^{2+}-dependent target cell killing of cytotoxic CD8$^+$ T lymphocytes (CTL) and natural killer (NK) cells protects the human body against infection and tumor formation. Orai and STIM proteins have been identified as key components of store-operated Ca^{2+}-influx. In addition, several modulators of SOCE (store-operated calcium entry) have been published (see below). However, it is not clear how intracellular Ca^{2+} in CTL is regulated with respect to optimal killing efficiency. Thus, it is important to identify new proteins.

To illustrate the importance of the identification of new proteins involved in cytotoxicity further, we would like to stress the example of PD-1, which is a very important surface receptor known to inhibit cytotoxic immune cell function (Sharpe and Pauken, 2018). PD-1/PD-L1 interaction results in T cell exhaustion which is one of the major problems for immunotherapy. The success of the PD-1/PD-L1 immune checkpoint blockade by different anti-PD-1/PD-L1 antibodies for immune therapy is based on this principle to evade T cell exhaustion and T cell blockade (reviewed in Budimir et al., 2022). This example highlights how identification of new proteins/pathways involved in cytotoxicity may revolutionize immune therapy.

In this study, we screened candidates suggested from bioinformatics gene prioritization in a real-time killing assay and identified four hits

CCR5, KCNN4, RCAN3 and BCL2 modifying CTL cytotoxicity. CTL cytotoxicity is indeed of great clinical relevance in conjunction with CAR T-cell immunotherapy. Identification of molecules involved in this process might have the potential for future trials to develop diagnostic markers that may predict the responsiveness of CTL activation to calcium for particular patients (in the direction of personalized medicine) to optimize the clinical outcome in the future.

4.1. Hits identified in this study

1. KCNN4

   KCNN4 codes for the Ca^{2+}-activated potassium channel $K_{Ca}3.1$ (also known as $IKCa^{2+}$ or SK4). $K_{Ca}3.1$ is a well-studied ion channel in immune cells and especially in T-cells. For this reason, its function has already been extensively explored and reviewed (among others: (Feske et al., 2012; Lewis and Cahalan, 1995; Panyi et al., 2004; Trebak and Kinet, 2019; Xiao et al., 2003). $K_{Ca}3.1$ activity is mediated by Ca^{2+}-binding to pre-bound calmodulin and the subsequent K^+-efflux preserves the negative membrane potential required as driving force for sustained Ca^{2+}-influx (Fanger et al., 1999). The compartmentalization of $K_{Ca}3.1$ to the immunological synapse upon T-cell activation as a part of the signaling complex facilitates proliferation and cytokine production (Nicolaou et al., 2007) and also suggests a role for modulating the optimal $[Ca^{2+}]$ necessary for killing of CTL. Since the down-regulation of *KCNN4* mRNA was only about 50%, it is not surprising that we could not identify any effect on killing in SEA-CTL in culture medium (AIMV) with a free $[Ca^{2+}]$ of about 0.8 mM (X. Zhou et al., 2018). However, reducing the extracellular $[Ca^{2+}]$ down to 11 μM (corresponding to the addition of 0.93 mM EGTA, (X. Zhou et al., 2018)), we found a severe reduction in killing capacity suggesting a role for KCa3.1 in preserving optimal $[Ca^{2+}]$. In accordance, in case extracellular $[Ca^{2+}]$ was not limited, we only found a less-pronounced reduction in killing capacity using the $K_{Ca}3.1$-inhibitor TRAM34 which blocks $K_{Ca}3.1$ ion channel activity but not its compartmentalization within the IS (Nicolaou et al., 2007; Wulff et al., 2000). Interestingly, the effect of reducing killing capacity with the application of TRAM34 was much more pronounced in CTL-MART-1 compared to SEA-CTL (Figure 8). This is in a very good agreement with the fact that $K_{Ca}3.1$ expression is dramatically enhanced after T-cell activation (Grissmer et al., 1992), as SEA-CTL are less activated compared to CTL-MART-1.

2. RCAN3

   In vertebrates, three regulators (RCAN, previously called DSCR, MCIP, and calcipressin (CALP)) are known to regulate calcineurin activity (Serrano-Candelas et al., 2014). Out of these, the interaction between RCAN3 and calcineurin is caused by one single motif (CIC motif) and inhibits the Ca^{2+}-calcineurin mediated translocation of NFAT to the nucleus and thus T-cell activation (Mulero et al., 2009; Mulero et al., 2007). We observed no influence on killing in SEA-CTL in normal medium even though the down-regulation of RCAN3 mRNA was reasonably efficient (down to 30%). In CTL-MART-1, in which down-regulation by siRNA was more efficient (down to 18% compared to control siRNA transfected cells), the killing efficiency in RCAN3 siRNA transfected cells was significantly enhanced in culture medium (AIMV) with a free $[Ca^{2+}]$ of about 0.8 mM (X. Zhou et al., 2018), but only 48 h after siRNA transfection (compare Supplementary Figure 1). This suggests (which is not in a good agreement with (Klein-Hessling et al., 2017)) that less Ca^{2+}-calcineurin mediated translocation of NFAT to the nucleus is correlated with enhanced killing. However, we cannot exclude different, so far unknown, modes of action which were not the subject of this screening project.

3. CCR5

   The G-protein-coupled receptor, C-C chemokine receptor type 5 (CCR5) is the receptor for the β-chemokines chemokine ligand (CCL)-3 (MlP-lα), CCL4 (MIP-lβ), and CCL5 (RANTES). It is known for its central role in the entry of human immunodeficiency virus (HIV) infection into $CD4^+$ T-cells, by acting as co-receptor next to CD4 (Alkhatib et al., 1996; Deng et al., 1996). CCR5 expression in effector $CD8^+$ T-cells also seems to be correlated with proliferation, with the production of inflammatory cytokines such as TNFα, interleukin 2 (IL-2) or interferon (INF)-γ (Palmer et al., 2010) and with the migration to inflamed tissue (Fukada et al., 2002). Recently, in an increased number of activated $CD8^+$ T-cells, elevated expression levels of CCR5 (together with TNFR2) were identified in PBMC from glioma patients' peripheral blood (P. Y. Chen et al., 2019). Also, CCR5 was identified as a marker for natural killer T (NKT) cells (Liu et al., 2019). The FDA approved CCR5 inhibitor Maraviroc inhibits T-cell migration and at high concentrations (100 μM) also proliferation (Arberas et al., 2013). Interestingly, when inhibiting CCR5 with Maraviroc in CTL-MART-1, the killing efficiency was slightly reduced which might be associated with a lower production of inflammatory cytokines.

4. BCL2

   Bcl-2 belongs to the Bcl-2 family proteins which are documented as regulators of apoptosis in the mitochondrial pathway existing of pro- and anti-apoptotic members (Popgeorgiev et al., 2018). Bcl-2 is an anti-apoptotic, pro-survival member of this family. It plays a central role in B-cell lymphoma development (Adams et al., 2018) with gene translocations in 90% of follicular lymphoma (FL) and in 20% of diffuse large B-cell lymphoma (DLBCL) (Kahl and Yang, 2016; Schuetz et al., 2012). In the scenario of (relapsed) chronic lymphocytic leukemia (CLL), Bcl-2 is substantially over-expressed which leads to long-lived clonal lymphocytes (Robertson et al., 1996). The administration of Venetoclax, a specific inhibitor of Bcl-2, has improved outcomes for the patients (Roberts et al., 2016). More recently, there are also ongoing studies in which Venetoclax is administered in combination with obinutuzumab (anti-CD20 antibody) (summarized in (Salvaris and Opat, 2020)).

   Apart from its important role in B-cell lymphoma, Bcl-2 was also shown to directly regulate the intracellular Ca^{2+} level by inhibiting the inositol 1,4,5-trisphosphate ($InsP_3$) receptor-mediated Ca^{2+}-influx (R. Chen et al., 2004). Already 25 years ago, it was discovered that Bcl-2 influences the Ca^{2+}-homeostasis (also in the context of its partial localization to the mitochondrial membrane) (Baffy et al., 1993; Lam et al., 1994; Magnelli et al., 1994) but its effect on the regulation of Ca^{2+} in the ER lumen is controversially discussed (Distelhorst and Shore, 2004). Lee and his colleagues reported a protective function of Bcl-2 in the target cells p815 against Fas- but not perforin-mediated lysis of CTL (Lee et al., 1996). However, to our knowledge the Bcl-2 effect on killing efficiency has not been investigated yet. Inhibition of Bcl-2 with Venetoclax significantly decreased killing efficiency of CTL-MART-1, pointing to a Ca^{2+}-regulating function in these cells.

4.2. Candidates which have been not identified in this study

In fact, many other molecules are known to regulate Ca^{2+}-homeostasis in T-cells in general but also in $CD8^+$ T-cells. Among them are: plasma membrane Ca^{2+} ATPases (PMCA), sarcoplasmic/endoplasmic reticulum Ca^{2+} ATPase (SERCA), mitochondrial Ca^{2+} uniporter (MCU), transient receptor potential (TRP) channels, purinergic ionotropic receptors (P2RXs), voltage-activated Ca^{2+} (CaV) channels, P2RXs (P2RX1, P2RX4 or P2RX7) or Piezo channels which are gated by mechanical stimuli. Many excellent and elaborate reviews summarize the function of these proteins in T-cells (Cahalan and Chandy, 2009; Cahalan et al., 2001; Feske, 2007; Feske et al., 2012; Lewis, 2001; Nohara et al., 2015; Oh-hora and Rao, 2008; Trebak and Kinet, 2019; Vaeth and Feske, 2018). Our strict selection criteria (DEG expressed between NK cells and SEA-CTL, excluding genes which were already DEG between un-stimulated $CD8^+$ T-cells and SEA-CTL, reasonable expression level in SEA-CTL), resulted in only 29 candidates. This means that we likely did

not identify all candidates which regulate Ca^{2+}-homeostasis and therefore could also potentially regulate the killing function in NK cells or CTL.

4.3. Conclusions

In summary, based on modern transcriptomic analysis of microarray-based expression data of CTL and NK cells, we narrowed in on a small panel of 31 candidate genes that possibly regulate the Ca^{2+}-homeostasis in CTL. Due to the small number of candidates, we were able to screen them in detail in primary human cells by siRNA-directed silencing. We identified clear, reproducible effects of four candidate genes on killing efficiency in case the killing assay was performed in clonal CTL-MART-1 under Ca^{2+}-limiting conditions that put selective pressure on Ca^{2+}-regulation. Our findings were validated in an orthogonal screen by applying small-molecule inhibitors of the candidate proteins. Hence, this study successfully identified four molecular players, KCNN4, RCAN3, CCR5 and BCL2, that regulate Ca^{2+} dependent killing capacity of CD8$^+$ T-cells.

Ethical approval

The use of residual human material was approved by the local ethics committee (Ärztekammer des Saarlandes, reference 84/15, Prof. Dr. Rettig-Stürmer).

Funding

This work was funded by the Deutsche Forschungsgemeinschaft (DFG, the collaborative research centers SFB 1027 (project A11 to MH, project C3 to VH) and SFB 894 (project A1 to MH)).

Additional information

A preprint of this manuscript has previously been published (Zöphel et al., 2021).

Author agreement

All authors have seen and approved the final version of the revised manuscript.

CRediT authorship contribution statement

S.Z., Ma.H., Mo.H., V.H., E.C.S. designed the study. **S.Z., G.S., V.K., C.H.** designed and performed experiments. M**o.H., M.N.** performed the data pre-processing, the computational framework and analyzed the data. **E.M.** contributed to the microarray experiments. **S.Z., E.C.S.** coordinated data analyses and designed final figure layout. **M.N.** contributed Supplementary Figure 1. **E.C.S.** wrote the manuscript in consultation with **S.Z., Ma.H., V.H.** and contribution by **Mo.H., M.N.** All authors carefully checked the manuscript and provided critical feedback.

Declaration of Competing Interest

The authors declare no competing or conflicting interests.

Data availability

Microarray data supporting the findings of this study are openly available at the GEO platform (https://www.ncbi.nlm.nih.gov/geo/) under the accession number GSE168692.

Appendix A. Supporting information

Supplementary data associated with this article can be found in the online version at doi:10.1016/j.molimm.2023.04.002.

References

Adams, C.M., Clark-Garvey, S., Porcu, P., Eischen, C.M., 2018. Targeting the Bcl-2 Family in B Cell Lymphoma. Front. Oncol. 8, 636.

Alkhatib, G., Combadiere, C., Broder, C.C., Feng, Y., Kennedy, P.E., Murphy, P.M., Berger, E.A., 1996. CC CKR5: a RANTES, MIP-1alpha, MIP-1beta receptor as a fusion cofactor for macrophage-tropic HIV-1. Science 272, 1955–1958.

Arberas, H., Guardo, A.C., Bargallo, M.E., Maleno, M.J., Calvo, M., Blanco, J.L., Garcia, F., Gatell, J.M., Plana, M., 2013. In vitro effects of the CCR5 inhibitor maraviroc on human T cell function. J. Antimicrob. Chemother. 68, 577–586.

Badou, A., Jha, M.K., Matza, D., Flavell, R.A., 2013. Emerging roles of L-type voltage-gated and other calcium channels in T lymphocytes. Front. Immunol. 4, 243.

Baffy, G., Miyashita, T., Williamson, J.R., Reed, J.C., 1993. Apoptosis induced by withdrawal of interleukin-3 (IL-3) from an IL-3-dependent hematopoietic cell line is associated with repartitioning of intracellular calcium and is blocked by enforced Bcl-2 oncoprotein production. J. Biol. Chem. 268, 6511–6519.

Bellucci, R., Nguyen, H.N., Martin, A., Heinrichs, S., Schinzel, A.C., Hahn, W.C., Ritz, J., 2012. Tyrosine kinase pathways modulate tumor susceptibility to natural killer cells. J. Clin. Investig. 122, 2369–2383.

Bhat, S.S., Friedmann, K.S., Knorck, A., Hoxha, C., Leidinger, P., Backes, C., Meese, E., Keller, A., Rettig, J., Hoth, M., Qu, B., Schwarz, E.C., 2016. Syntaxin 8 is required for efficient lytic granule trafficking in cytotoxic T lymphocytes. Biochim. Biophys. Acta 1863, 1653–1664.

Budimir, N., Thomas, G.D., Dolina, J.S., Salek-Ardakani, S., 2022. Reversing T-cell exhaustion in cancer: lessons learned from PD-1/PD-L1 immune checkpoint blockade. Cancer Immunol. Res. 10, 146–153.

Cahalan, M.D., Chandy, K.G., 2009. The functional network of ion channels in T lymphocytes. Immunol. Rev. 231, 59–87.

Cahalan, M.D., Wulff, H., Chandy, K.G., 2001. Molecular properties and physiological roles of ion channels in the immune system. J. Clin. Immunol. 21, 235–252.

Chen, P.Y., Wu, C.Y., Fang, J.H., Chen, H.C., Feng, L.Y., Huang, C.Y., Wei, K.C., Fang, J.Y., Lin, C.Y., 2019. Functional change of effector tumor-infiltrating CCR5(+)CD38(+)HLA-DR(+)CD8(+) T cells in glioma microenvironment. Front. Immunol. 10, 2395.

Chen, R., Valencia, I., Zhong, F., McColl, K.S., Roderick, H.L., Bootman, M.D., Berridge, M.J., Conway, S.J., Holmes, A.B., Mignery, G.A., Velez, P., Distelhorst, C.W., 2004. Bcl-2 functionally interacts with inositol 1,4,5-trisphosphate receptors to regulate calcium release from the ER in response to inositol 1,4,5-trisphosphate. J. Cell Biol. 166, 193–203.

Deng, H., Liu, R., Ellmeier, W., Choe, S., Unutmaz, D., Burkhart, M., Di Marzio, P., Marmon, S., Sutton, R.E., Hill, C.M., Davis, C.B., Peiper, S.C., Schall, T.J., Littman, D.R., Landau, N.R., 1996. Identification of a major co-receptor for primary isolates of HIV-1. Nature 381, 661–666.

Distelhorst, C.W., Shore, G.C., 2004. Bcl-2 and calcium: controversy beneath the surface. Oncogene 23, 2875–2880.

Fanger, C.M., Ghanshani, S., Logsdon, N.J., Rauer, H., Kalman, K., Zhou, J., Beckingham, K., Chandy, K.G., Cahalan, M.D., Aiyar, J., 1999. Calmodulin mediates calcium-dependent activation of the intermediate conductance KCa channel IKCa1. J. Biol. Chem. 274, 5746–5754.

Fenninger, F., Jefferies, W.A., 2019. What's Bred in the Bone: Calcium Channels in Lymphocytes. J. Immunol. 202, 1021–1030.

Feske, S., 2007. Calcium signalling in lymphocyte activation and disease. Nat. Rev. Immunol. 7, 690–702.

Feske, S., 2013. Ca(2+) influx in T cells: how many ca(2+) channels? Front. Immunol. 4, 99.

Feske, S., Skolnik, E.Y., Prakriya, M., 2012. Ion channels and transporters in lymphocyte function and immunity. Nat. Rev. Immunol. 12, 532–547.

Friedmann, K.S., Bozem, M., Hoth, M., 2019. Calcium signal dynamics in T lymphocytes: comparing in vivo and in vitro measurements. Semin. Cell Dev. Biol. 94, 84–93.

Friedmann, K.S., Kaschek, L., Knörck, A., Cappello, S., Lünsmann, N., Küchler, N., Hoxha, C., Schäfer, G., Iden, S., Bogeski, I., Kummerow, C., Schwarz, E.C., Hoth, M., 2022. Interdependence of sequential cytotoxic T lymphocyte and natural killer cell cytotoxicity against melanoma cells. J. Physiol. 600, 5027–5054.

Fukada, K., Sobao, Y., Tomiyama, H., Oka, S., Takiguchi, M., 2002. Functional expression of the chemokine receptor CCR5 on virus epitope-specific memory and effector CD8 + T cells. J. Immunol. 168, 2225–2232.

Grissmer, S., Lewis, R.S., Cahalan, M.D., 1992. Ca(2+)-activated K+ channels in human leukemic T cells. J. Gen. Physiol. 99, 63–84.

Hamed, M., Spaniol, C., Zapp, A., Helms, V., 2015. Integrative network-based approach identifies key genetic elements in breast invasive carcinoma. BMC Genom. 16 (Suppl 5), S2.

Hattab, D., Bakhtiar, A., 2020. Bioengineered siRNA-Based nanoplatforms targeting molecular signaling pathways for the treatment of triple negative breast cancer: preclinical and clinical advancements. Pharmaceutics 12.

Hochberg, Y., Benjamini, Y., 1990. More powerful procedures for multiple significance testing. Stat. Med. 9, 811–818.

Ihaka, R., Gentleman, R., 1996. R: a language for data analysis and graphics. J. Comput. Graph. Stat. 5, 299–314.

Kahl, B.S., Yang, D.T., 2016. Follicular lymphoma: evolving therapeutic strategies. Blood 127, 2055–2063.

Kanehisa, M., Sato, Y., Kawashima, M., Furumichi, M., Tanabe, M., 2016. KEGG as a reference resource for gene and protein annotation. Nucleic Acids Res. 44, D457–D462.

Khandelwal, N., Breinig, M., Speck, T., Michels, T., Kreutzer, C., Sorrentino, A., Sharma, A.K., Umansky, L., Conrad, H., Poschke, I., Offringa, R., König, R., Bernhard, H., Machlenkin, A., Boutros, M., Beckhove, P., 2015. A high-throughput RNAi screen for detection of immune-checkpoint molecules that mediate tumor resistance to cytotoxic T lymphocytes. EMBO Mol. Med. 7, 450–463.

Klein-Hessling, S., Muhammad, K., Klein, M., Pusch, T., Rudolf, R., Floter, J., Qureischi, M., Beilhack, A., Vaeth, M., Kummerow, C., Backes, C., Schoppmeyer, R., Hahn, U., Hoth, M., Bopp, T., Berberich-Siebelt, F., Patra, A., Avots, A., Muller, N., Schulze, A., Serfling, E., 2017. NFATc1 controls the cytotoxicity of CD8(+) T cells. Nat. Commun. 8, 511.

Knorck, A., Marx, S., Friedmann, K.S., Zophel, S., Lieblang, L., Hassig, C., Muller, I., Pilch, J., Sester, U., Hoth, M., Eichler, H., Sester, M., Schwarz, E.C., 2018. Quantity, quality, and functionality of peripheral blood cells derived from residual blood of different apheresis kits. Transfusion 58, 1516–1526.

Kummerow, C., Schwarz, E.C., Bufe, B., Zufall, F., Hoth, M., Qu, B., 2014. A simple economic time-resolved killing assay. Eur. J. Immunol. 44, 1870–1872.

Lam, M., Dubyak, G., Chen, L., Nunez, G., Miesfeld, R.L., Distelhorst, C.W., 1994. Evidence that BCL-2 represses apoptosis by regulating endoplasmic reticulum-associated Ca2+ fluxes. Proc. Natl. Acad. Sci. 91, 6569–6573.

Lee, R.K., Spielman, J., Podack, E.R., 1996. Bcl-2 protects against Fas-based but not perforin-based T cell-mediated cytolysis. Int. Immunol. 8, 991–1000.

Lewis, R.S., 2001. Calcium signaling mechanisms in T lymphocytes. Annu Rev. Immunol. 19, 497–521.

Lewis, R.S., Cahalan, M.D., 1995. Potassium and calcium channels in lymphocytes. Annu Rev. Immunol. 13, 623–653.

Liu, J., Hill, B.J., Darko, S., Song, K., Quigley, M.F., Asher, T.E., Morita, Y., Greenaway, H.Y., Venturi, V., Douek, D.C., Davenport, M.P., Price, D.A., Roederer, M., 2019. The peripheral differentiation of human natural killer T cells. Immunol. Cell Biol. 97, 586–596.

Magnelli, L., Cinelli, M., Turchetti, A., Chiarugi, V.P., 1994. Bcl-2 overexpression abolishes early calcium waving preceding apoptosis in NIH-3T3 murine fibroblasts. Biochem. Biophys. Res. Commun. 204, 84–90.

Mainini, F., Eccles, M.R., 2020. Lipid and polymer-based nanoparticle sirna delivery systems for cancer therapy. Molecules 25.

Mantei, A., Rutz, S., Janke, M., Kirchhoff, D., Jung, U., Patzel, V., Vogel, U., Rudel, T., Andreou, I., Weber, M., Scheffold, A., 2008. siRNA stabilization prolongs gene knockdown in primary T lymphocytes. Eur. J. Immunol. 38, 2616–2625.

Martens, M., Ammar, A., Riutta, A., Waagmeester, A., Slenter, D.N., Hanspers, K., R, A. M., Digles, D., Lopes, E.N., Ehrhart, F., Dupuis, L.J., Winckers, L.A., Coort, S.L., Willighagen, E.L., Evelo, C.T., Pico, A.R., Kutmon, M., 2020. WikiPathways: connecting communities. Nucleic Acids Res.

Maul-Pavicic, A., Chiang, S.C., Rensing-Ehl, A., Jessen, B., Fauriat, C., Wood, S.M., Sjoqvist, S., Hufnagel, M., Schulze, I., Bass, T., Schamel, W.W., Fuchs, S., Pircher, H., McCarl, C.A., Mikoshiba, K., Schwarz, K., Feske, S., Bryceson, Y.T., Ehl, S., 2011. ORAI1-mediated calcium influx is required for human cytotoxic lymphocyte degranulation and target cell lysis. Proc. Natl. Acad. Sci. 108, 3324–3329.

Moffat, J., Sabatini, D.M., 2006. Building mammalian signalling pathways with RNAi screens. Nat. Rev. Mol. Cell Biol. 7, 177–187.

Mulero, M.C., Aubareda, A., Schluter, A., Perez-Riba, M., 2007. RCAN3 a novel calcineurin inhibitor that down-regulates NFAT-dependent cytokine gene expression. Biochim. Biophys. Acta 1773, 330–341.

Mulero, M.C., Aubareda, A., Orzaez, M., Messeguer, J., Serrano-Candelas, E., Martinez-Hoyer, S., Messeguer, A., Perez-Paya, E., Perez-Riba, M., 2009. Inhibiting the calcineurin-NFAT (nuclear factor of activated T cells) signaling pathway with a regulator of calcineurin-derived peptide without affecting general calcineurin phosphatase activity. J. Biol. Chem. 284, 9394–9401.

Nazarieh, M., Helms, V., 2019. TopControl: a tool to prioritize candidate disease-associated genes based on topological network features. Sci. Rep. 9, 19472.

Nazarieh, M., Wiese, A., Will, T., Hamed, M., Helms, V., 2016. Identification of key player genes in gene regulatory networks. BMC Syst. Biol. 10, 88.

Nicolaou, S.A., Neumeier, L., Peng, Y., Devor, D.C., Conforti, L., 2007. The Ca(2+)-activated K(+) channel KCa3.1 compartmentalizes in the immunological synapse of human T lymphocytes. Am. J. Physiol. Cell Physiol. 292, C1431–C1439.

Nohara, L.L., Stanwood, S.R., Omilusik, K.D., Jefferies, W.A., 2015. Tweeters woofers and horns: the complex orchestration of calcium currents in T lymphocytes. Front. Immunol. 6, 234.

Oh-hora, M., Rao, A., 2008. Calcium signaling in lymphocytes. Curr. Opin. Immunol. 20, 250–258.

Palmer, L.A., Sale, G.E., Balogun, J.I., Li, D., Jones, D., Molldrem, J.J., Storb, R.F., Ma, Q., 2010. Chemokine receptor CCR5 mediates alloimmune responses in graft-versus-host disease. Biol. Blood Marrow Transpl. 16, 311–319.

Panyi, G., Varga, Z., Gaspar, R., 2004. Ion channels and lymphocyte activation. Immunol. Lett. 92, 55–66.

Pelletier, L., Savignac, M., 2013. Ca(2+) signaling in T-cell subsets with a focus on the role of cav1 channels: possible implications in therapeutics. Front. Immunol. 4, 150.

Popgeorgiev, N., Jabbour, L., Gillet, G., 2018. Subcellular localization and dynamics of the Bcl-2 family of proteins. Front. Cell Dev. Biol. 6, 13.

Roberts, A.W., Davids, M.S., Pagel, J.M., Kahl, B.S., Puvvada, S.D., Gerecitano, J.F., Kipps, T.J., Anderson, M.A., Brown, J.R., Gressick, L., Wong, S., Dunbar, M., Zhu, M., Desai, M.B., Cerri, E., Heitner Enschede, S., Humerickhouse, R.A., Wierda, W.G., Seymour, J.F., 2016. Targeting BCL2 with venetoclax in relapsed chronic lymphocytic leukemia. N. Engl. J. Med. 374, 311–322.

Robertson, L.E., Plunkett, W., McConnell, K., Keating, M.J., McDonnell, T.J., 1996. Bcl-2 expression in chronic lymphocytic leukemia and its correlation with the induction of apoptosis and clinical outcome. Leukemia 10, 456–459.

Salvaris, R., Opat, S., 2020. An update of venetoclax and obinutuzumab in chronic lymphocytic leukemia. Future Oncol.

Schuetz, J.M., Johnson, N.A., Morin, R.D., Scott, D.W., Tan, K., Ben-Nierah, S., Boyle, M., Slack, G.W., Marra, M.A., Connors, J.M., Brooks-Wilson, A.R., Gascoyne, R.D., 2012. BCL2 mutations in diffuse large B-cell lymphoma. Leukemia 26, 1383–1390.

Serrano-Candelas, E., Farre, D., Aranguren-Ibanez, A., Martinez-Hoyer, S., Perez-Riba, M., 2014. The vertebrate RCAN gene family: novel insights into evolution structure and regulation. PLoS One 9, e85539.

Sharpe, A., Pauken, K., 2018. The diverse functions of the PD1 inhibitory pathway. Nat. Rev. Immunol. 18, 153–167. Epub 2017 Nov 13.

Shih, T., De, S., Barnes, B.J., 2019. RNAi transfection optimized in primary naive B cells for the targeted analysis of human plasma cell differentiation. Front Immunol. 10, 1652.

Sioud, M., 2020. Optimized siRNA delivery into Primary Immune Cells Using Electroporation. Methods Mol. Biol. 2115, 119–131.

Smith, N., Vidalain, P.O., Nisole, S., Herbeuval, J.P., 2016. An efficient method for gene silencing in human primary plasmacytoid dendritic cells: silencing of the TLR7/IRF-7 pathway as a proof of concept. Sci. Rep. 6, 29891.

The Gene Ontology, C, 2019. The gene ontology resource: 20 years and still going strong. Nucleic Acids Res. 47, D330–D338.

Trebak, M., Kinet, J.P., 2019. Calcium signalling in T cells. Nat. Rev. Immunol. 19, 154–169.

Vaeth, M., Feske, S., 2018. Ion channelopathies of the immune system. Curr. Opin. Immunol. 52, 39–50.

Wenning, A.S., Neblung, K., Strauss, B., Wolfs, M.J., Sappok, A., Hoth, M., Schwarz, E.C., 2011. TRP expression pattern and the functional importance of TRPC3 in primary human T-cells. Biochim. Et. Biophys. Acta 1813, 412–423.

Wulff, H., Miller, M.J., Hansel, W., Grissmer, S., Cahalan, M.D., Chandy, K.G., 2000. Design of a potent and selective inhibitor of the intermediate-conductance Ca2+-activated K+ channel, IKCa1: a potential immunosuppressant. Proc. Natl. Acad. Sci. 97, 8151–8156.

Xiao, L., Fu, H.Y., Song, D.M., Fan, S.G., 2003. [Ion channels on T lymphocyte]. Sheng Li Ke Xue Jin Zhan 34, 105–110.

Yao, D., Wang, J., Lu, Y., Noble, N., Sun, H., Zhu, X., Lin, N., Payan, D.G., Li, M., Qu, K., 2004. PathwayFinder: paving the way towards automatic pathway extraction proceedings of the second conference on Asia-Pacific bioinformatics. In: Australian Computer Society, Inc, Volume 29. Dunedin, New Zealand, pp. 53–62.

Zhou, L.Y., Qin, Z., Zhu, Y.H., He, Z.Y., Xu, T., 2019. Current RNA-based therapeutics in clinical trials. Curr. Gene Ther. 19, 172–196.

Zhou, P., Shaffer, D.R., Alvarez Arias, D.A., Nakazaki, Y., Pos, W., Torres, A.J., Cremasco, V., Dougan, S.K., Cowley, G.S., Elpek, K., Brogdon, J., Lamb, J., Turley, S. J., Ploegh, H.L., Root, D.E., Love, J.C., Dranoff, G., Hacohen, N., Cantor, H., Wucherpfennig, K.W., 2014. In vivo discovery of immunotherapy targets in the tumour microenvironment. Nature 506, 52–57.

Zhou, X., Friedmann, K.S., Lyrmann, H., Zhou, Y., Schoppmeyer, R., Knorck, A., Mang, S., Hoxha, C., Angenendt, A., Backes, C.S., Mangerich, C., Zhao, R., Cappello, S., Schwar, G., Hassig, C., Neef, M., Bufe, B., Zufall, F., Kruse, S., Niemeyer, B.A., Lis, A., Qu, B., Kummerow, C., Schwarz, E.C., Hoth, M., 2018. A calcium optimum for cytotoxic T lymphocyte and natural killer cell cytotoxicity. J. Physiol. 596, 2681–2698.

Zöphel, S., Schwär, G., Nazarieh, M., Konetzki, V., Hoxha, C., Meese, E., Hoth, M., Helms, V., Hamed, M., Schwarz, E.C., 2021. Identification of molecular candidates which regulate calcium-dependent CD8+ T-cell cytotoxicity. bioRxiv, 2020.2012.2022.423945.